J. Chem. Soc., Faraday Trans. 1, 1982, **78**, 1279-1290

Electroreduction of Alkali Metal Cations

Part 2.—Effects of Electrode Composition

BY ANDRZEJ S. BARANSKI AND W. RONALD FAWCETT*

Guelph–Waterloo Centre for Graduate Work in Chemistry (Guelph Campus), Department of Chemistry, University of Guelph, Guelph, Ontario N1G 2W1, Canada

Received 25th June, 1981

Kinetic data for the electroreduction of alkali metal cations in dimethylformamide and acetonitrile are reported at a variety of indium amalgam electrodes and at a gallium–indium electrode (eutectic composition). The kinetic parameters were found to depend markedly on the nature of the electrode material in which the product alkali metal is soluble. The data are discussed on the basis of a model in which adsorption of the metal cation on the electrode and transfer of the cation from the solution phase to the metal phase are assumed to be the rate-controlling steps. This model provides an excellent description of the variation in the kinetic parameters with electrode composition and potential.

It was shown in previous work[1, 2] that the kinetic parameters for the electroreduction of alkali metal cations at liquid electrodes, namely the standard rate constant and apparent transfer coefficient, are strongly dependent on the composition of both the solution and the electrode. The effect of solution composition can be related to changes in the solvent, and to changes in the electrostatic environment at the reaction site with change in the nature of the predominant counter-ion in the double layer.[2] A detailed model for the electrode process was proposed in which the rate-determining steps under most circumstances are adsorption of the reactant cation on the electrode surface and transfer of the adsorbed species from the solution phase to the electrode phase.

When the nature of the electrode is changed from pure mercury to another inert metal, the electrode reaction will be affected in at least two ways: (i) the free-energy profile for the rate-determining step is altered due to the change in free energy of the product in the metal, and (ii) the electrostatic environment in the solution is changed at constant electrode potential due to the corresponding change in the potential of zero charge (p.z.c.).[3, 4] The purpose of the present paper is to present in detail kinetic data obtained at a variety of liquid-metal electrodes and compare them with those obtained at pure mercury. The significance of the results within the context of the previously proposed model is discussed.

EXPERIMENTAL

The techniques used to obtain the kinetic data and the method of data analysis were described in Part 1.[2] In addition, the nature and construction of the working, counter and reference electrodes were given, as were the methods of purifying solvents and salts.[2]

Indium amalgam with a concentration of 70 atomic % In was prepared by dissolving a known weight of In (99.999%) in triply distilled Hg. Further purification of the amalgam was achieved by immersing it in a stirred solution of $In(ClO_4)_3$ for 8 h to dissolve more easily oxidized impurities. Amalgams of lower concentration were prepared by dilution with triply distilled Hg.

The indium–gallium alloy eutectic composition was also prepared by combining the appropriate amounts of the two metals (16.7 at. % In). It was immersed in a stirred solution of 0.01 mol dm^{-3} HCl for the same period. The alloys were washed with triply distilled water, followed by purified methanol and acetonitrile (AN) and stored under AN. These materials were handled in a controlled atmosphere chamber in the absence of oxygen and water. The dropping electrode was constructed in a column glass capillary 50 cm high to avoid using a large amount of the alloy material.

RESULTS

D.C. POLAROGRAPHY AND CYCLIC VOLTAMMETRY

D.c. polarography with a dropping amalgam electrode containing various atomic fractions of indium ($X_{In} = 0.035$, 0.07, 0.15, 0.3, 0.5, 0.6 and 0.7) was used to study the reduction of Li^+ in AN and dimethylformamide (DMF) and of Na^+ in DMF. The

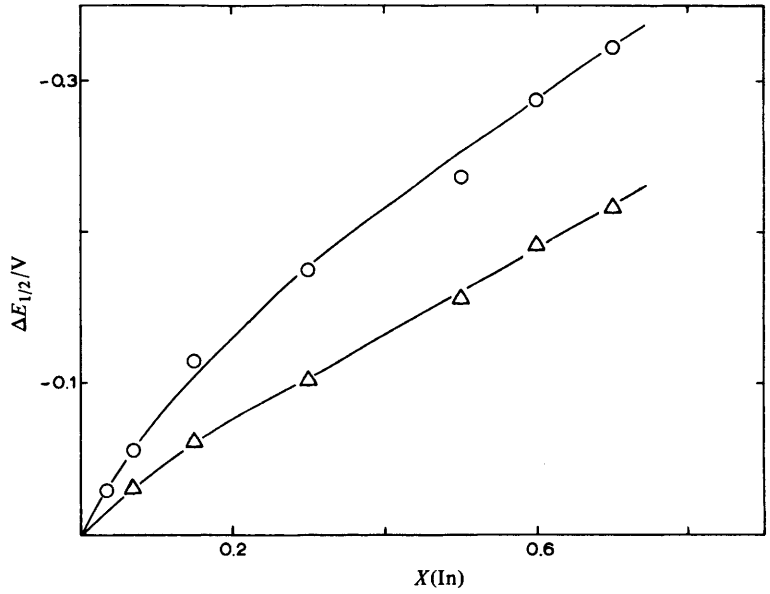

FIG. 1.—Shift in the half-wave potential for the reduction of Na^+ and Li^+ at an indium amalgam electrode from that at pure Hg, $\Delta E_{\frac{1}{2}}$ plotted against the atomic fraction of In in the amalgam X(In). The data for Na^+ were obtained in DMF with 0.25 mol dm^{-3} TEAP as electrolyte (○) and those for Li^+ in AN with 0.1 mol dm^{-3} TEAP (△).

reduction process was reversible in all cases, the half-wave potentials, $E_{\frac{1}{2}}$, being shifted in the negative direction with increase in In concentration. The shift in half-wave potential, $\Delta E_{\frac{1}{2}}$, for the reduction of Li^+ in AN with 0.1 mol dm^{-3} tetraethylammonium perchlorate (TEAP) and of Na^+ in DMF with 0.25 mol dm^{-3} TEAP is shown in fig. 1 as a function of In concentration. $\Delta E_{\frac{1}{2}}$ was assumed to be a function of the nature of the reactant and In concentration and to be independent of the nature of the solvent and electrolyte. The reduction of Na^+ in DMF at the Ga–In alloy was also reversible by d.c. polarography, $\Delta E_{\frac{1}{2}}$ being −0.49 V. However, the polarographic wave for Li^+ reduction at this alloy was deformed, probably because of the formation of solid intermetallic compounds in the electrode.

The reduction of Na^+ was also studied by cyclic voltammetry at a hanging-drop

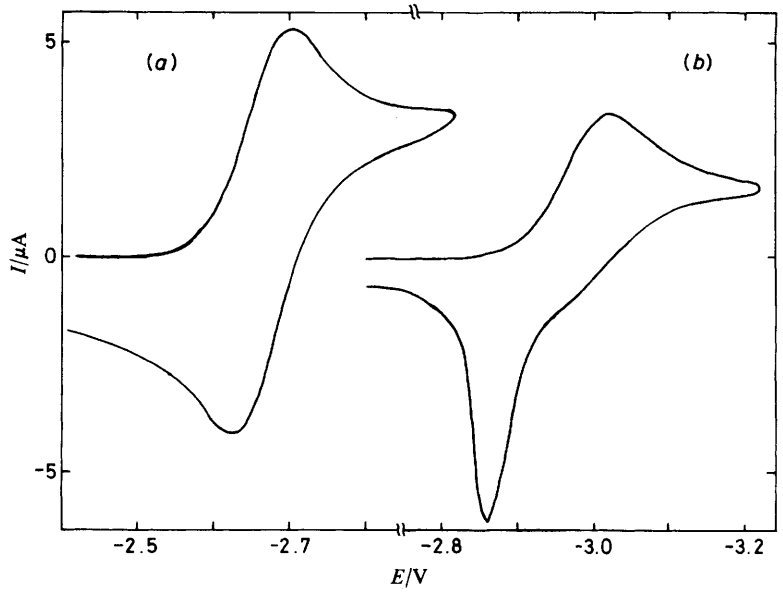

FIG. 2.—Cyclic voltammograms for the reduction of Na^+ in DMF containing 0.25 mol dm^{-3} TEAP at (*a*) an indium amalgam electrode containing 30 at. % In and (*b*) a Ga–In electrode of the eutectic composition.

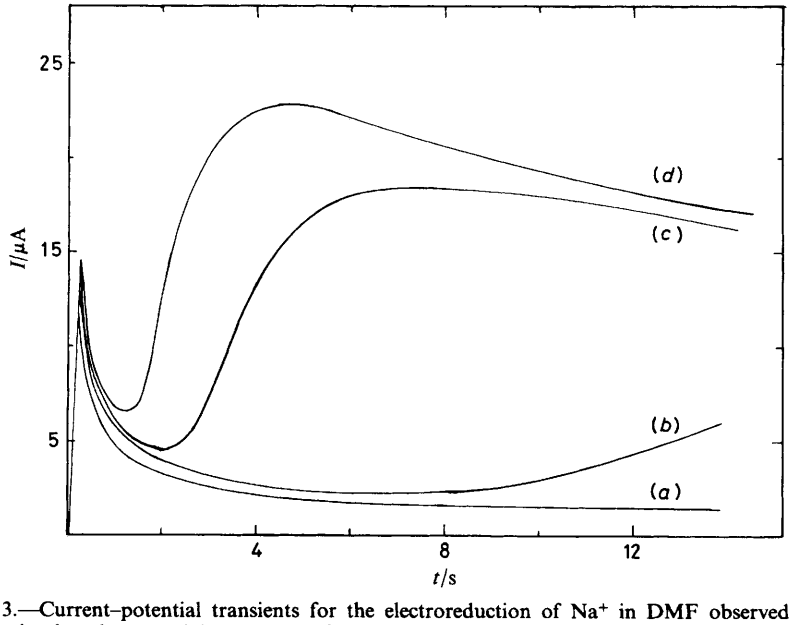

FIG. 3.—Current–potential transients for the electroreduction of Na^+ in DMF observed at a Ga–In electrode when the potential was stepped from a value where no faradaic current was flowing to a potential at the foot of the reduction wave. The final potentials and corresponding Na concentrations in the electrode calculated on the basis of the Nernst equation are (*a*) −2.87 V, ([Na] = 1.36×10^{-3} mol dm^{-3}), (*b*) −2.875 V, ([Na] = 1.65×10^{-3} mol dm^{-3}), (*c*) −2.880 V, ([Na] = 2.00×10^{-3} mol dm^{-3}) and (*d*) −2.890 V, ([Na] = 2.95×10^{-3} mol dm^{-3}). The potentials were measured against a Ag, Ag^+ reference electrode in the same solvent.[2]

electrode (Kemula type). In the case of indium amalgams (30 and 70 at. % In), the electrode process was reversible and diffusion controlled [fig. 2, curve (*a*)]. However, at the Ga–In alloy, the current–potential curve was much more complex [fig. 2, curve (*b*)], indicating the formation of an insoluble product. This conclusion was substantiated by means of current–time transients recorded after the potential was stepped from potentials where no faradaic current was flowing to values at the foot of the reduction wave for systems with high Na^+ concentration in solution (fig. 3). Similar curves were obtained previously for the reduction of Ni^{2+} at a hanging-mercury-drop electrode,[5] a system in which insoluble nickel–mercury compounds are formed. The character of the curves indicates that a supersaturated solution of Na is formed in the Ga–In alloy; after a certain critical concentration is reached in the induction period a precipitate is formed. On the basis of the current–time curves, it is estimated that the induction period is longer than 2 s for Na concentrations in the electrode less than 0.002 mol dm^{-3}. Thus, it may be assumed that the crystallization process does not affect the current–voltage curve for reduction of Na^+ at the Ga–In alloy under polarographic conditions (low Na^+ concentration and drop times of the order of a few seconds). Because of the low surface tension at the electrode/solution interface, hanging-drop electrodes can become unstable at far negative potentials and experimental work can be technically very difficult. Unfortunately, this electrode system could not be used to study the electroreduction of Li^+ since a complete current–voltage curve could not be registered before the hanging drop detached itself from the glass capillary support.

A.C. ADMITTANCE EXPERIMENTS

Kinetic parameters for the electroreduction of Li^+ and Na^+ in DMF and of Li^+ in AN were measured by the a.c. admittance technique described in Part 1.[2] The applicability of Randles' equivalent circuit for interfacial impedance was tested by comparing the value of the diffusion coefficient for the reactant in solution calculated from the Warburg impedance with that calculated from the diffusion-limited current observed in the d.c. polarogram. For all systems, except the reduction of Li^+ at the Ga–In alloy, the two values agreed within experimental error. In the case of the exception, the experimental value of the Warburg impedance was approximately four times smaller than that expected for the diffusion-controlled process, calculated on the basis of the diffusion coefficient estimated from d.c. polarography. As suggested above, the non-typical behaviour of this system indicates the presence of a chemical reaction following the charge-transfer process, probably the formation of a solid intermetallic compound.

Half-wave potentials were estimated from the position of the minimum in the out-of-phase component of the a.c. impedance after the data had been corrected for solution resistance and double-layer capacitance;[2] these values were in good agreement (± 2 mV) with those found by d.c. polarography. In many cases, there were significant differences between the peak potentials for the in-phase and out-of-phase components of the admittance. For example, in the case of electroreduction of Na^+ in DMF at 50 at. % indium amalgam, these peaks appeared at potentials separated by 25 mV at a frequency of 860 Hz. Such a separation is expected when the transfer coefficient is low ($\alpha \ll 0.5$). The standard rate constant was calculated from the values of in- and out-of-phase admittances at the half-wave potential, and the apparent transfer coefficient from the potential dependence of the rate constant in the vicinity of the half-wave potential. Kinetic data are recorded in table 1 for the systems studied at a 60 at. % In amalgam electrode in DMF. The same trends are observed at this electrode as are seen at Hg. First, for a given reactant, the standard rate constant and

apparent transfer coefficient increase with increasing size of the cation of the supporting electrolyte and the standard rate constant decreases with increasing electrolyte concentration. This result is illustrated in more detail in fig. 4 for the reduction of Na^+ in DMF at Hg and 60 at. % In amalgam. The change in log k_s for a given change in electrolyte concentration at the amalgam electrode is more than twice

TABLE 1.—KINETIC DATA FOR THE ELECTROREDUCTION OF ALKALI METAL CATIONS IN DMF AT A 60 at. % In AMALGAM ELECTRODE ($T = 25$ °C)

reactant	supporting electrolyte[a] /mol dm^{-3}	shift in half-wave potential, $\Delta E_{\frac{1}{2}}$/V	standard rate constant, k_s/cm s^{-1}	apparent transfer coefficient, α_a
Li^+	0.1, TEAP	−0.192	8.4×10^{-3}	0.43
	0.1, TPAP	−0.192	0.138	0.74
	0.1, TBAP	−0.192	0.622	0.93
Na^+	0.1, TEAP	−0.287	0.543	0.01
	0.25, TEAP	−0.287	0.153	0.06
K^+	0.25, TEAP	−0.362	0.350	0.07

[a] The supporting electrolytes were tetra-alkylammonium perchlorates (E = ethyl, P = propyl and B = butyl).

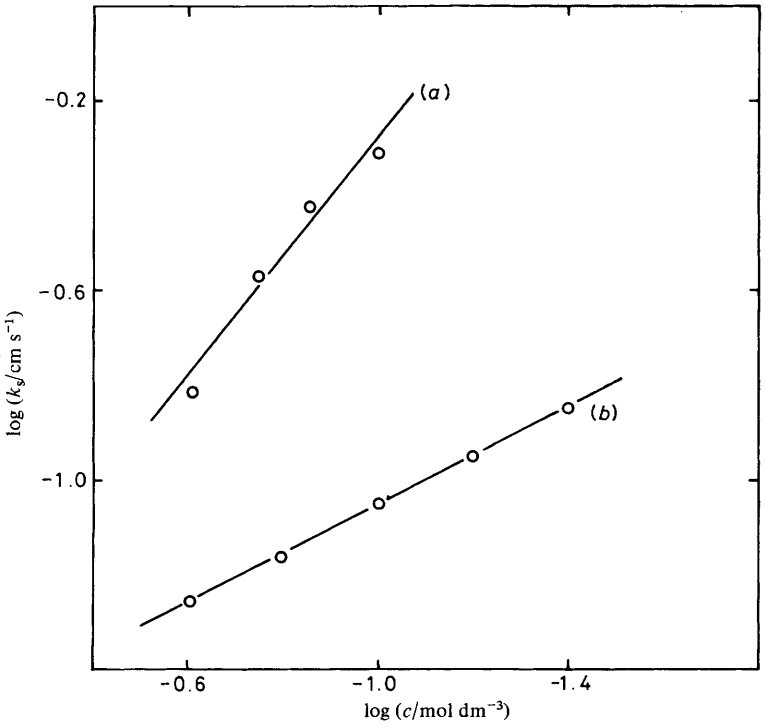

FIG. 4.—Plots of the logarithm of the standard rate constant for electroreduction of Na^+ in DMF (*a*) at 60 at. % In amalgam and (*b*) at Hg against the logarithm of the salt (TEAP) concentration.

that observed at Hg. On the basis of the classical theory of double-layer effects in electrode kinetics,[6] this result indicates that the apparent transfer coefficient for reduction at the amalgam is much less than at Hg and confirms the values of α_a measured from the potential dependence of the rate constant [table 1 and data reported in ref. (2)]. The third trend is an increase in standard rate constant with increase in alkali metal atomic number for a given supporting electrolyte. It is assumed to reflect a decrease in free energy of activation for the electrode process with decrease in reactant solvation.[1, 2]

TABLE 2.—KINETIC DATA FOR THE ELECTROREDUCTION OF ALKALI METAL CATIONS IN NON-AQUEOUS MEDIA AT A VARIETY OF LIQUID-METAL ELECTRODES ($T = 25$ °C)

reactant and solvent	supporting electrolyte /mol dm^{-3}	electrode composition	shift in half-wave potential, $\Delta E_{\frac{1}{2}}$/V	standard rate constant, k_2/cm s^{-1}	apparent transfer coefficient, α_a
Li^+ in DMF	0.1, TBAP	15 at. % In–Hg	−0.063	8.0×10^{-3}	0.71
		30 at. % In–Hg	−0.104	2.8×10^{-2}	0.75
Li^+ in AN	0.1, TEAP	7 at. % In–Hg	−0.032	6.5×10^{-2}	0.60
		15 at. % In–Hg	−0.063	0.173	0.52
		30 at. % In–Hg	−0.104	0.416	0.25
		50 at. % In–Hg	−0.156	0.540	0.28
		70 at. % In–Hg	−0.216	0.677	0.08
Na^+ in DMF	0.25, TEAP	3.5 at. % In–Hg	−0.029	9.4×10^{-2}	0.36
		7 at. % In–Hg	−0.055	0.127	0.27
		15 at. % In–Hg	−0.115	0.155	0.12
		30 at. % In–Hg	−0.175	0.147	0.03
		50 at. % In–Hg	−0.236	0.152	0.08
		70 at. % In–Hg	−0.322	0.146	0.08
		17 at. % In–Ga	−0.490	0.163	0.09

The results of experiments at other liquid-metal electrodes are summarized in table 2. These data demonstrate that the standard rate constant increases markedly with increase in indium content in the amalgam; at the same time, the apparent transfer coefficient decreases.[1] In the case of the reduction of Na^+ from a DMF solution, limiting values of k_s and α_a are reached. It is probable that the same would occur for the reduction of Li^+ but the limiting value of the standard rate constant would be outside of the range which can be measured by the usual experimental methods. Note that the increase in standard rate constant with indium concentration follows a corresponding decrease in free energy of solvation of the alkali metal in the electrode.

DISCUSSION

It is apparent from the data obtained that the electrode composition has a very marked effect on both the standard rate constant and apparent transfer coefficient for the electroreduction of alkali metal cations. These changes may be attributed to (*a*) changes in double-layer structure and (*b*) change in the solvation energy of the alkali metal product in the electrode.

In order to assess the first effect, one should have equilibrium double-layer data for the various liquid-metal electrodes in the non-aqueous solvents used. Very few data

exist for metals other than Hg in non-aqueous solutions.[7,8] Yakovleva and Nikolaeva-Fedorovich[9] obtained electrode charge density against potential data for indium amalgams in dilute aqueous solutions and showed that the charge density is almost independent of electrode potential for varying indium concentration at potentials more negative than -1.5 V against a normal calomel electrode. Bagotskaya *et al.*[10,11] have compared electrode charge density against potential curves in In–Ga alloys with those at Hg in dimethyl sulphoxide and AN. For these systems, there is a significant difference between the charge densities on the two metals at constant potential; however, the difference between the charge densities is constant in the potential region of interest. Thus, one may expect that the double-layer effect for the forward process changes by some constant amount when one changes the nature of the electrode, and that the potential dependence of this effect is independent of the nature of the electrode in the region of very negative potentials.

The mechanism proposed previously[2] for the reduction of alkali metal cations at electrodes in which the product is soluble is the following:

$$M^+(\text{bulk}) \rightleftharpoons M^+(\text{in d.l.}) \overset{1}{\rightleftharpoons} M^+(\text{ads.}) \overset{2}{\rightleftharpoons} M^+(\text{in electrode}) + e \overset{3}{\rightleftharpoons} M(\text{in electrode}). \quad (1)$$

On the basis of previously published data,[1,2,12,13] one expects either the adsorption process (step 1) or the metal-transfer process (step 2) to control the reaction in the forward direction. When step 1 is rate controlling, the free energy of activation is approximately independent of potential[2] and one observes apparent transfer coefficients close to zero. This result is obtained in the cases of the electroreduction of Na^+ and K^+ in hexamethylphosphoramide with tetrabutylammonium perchlorate (TBAP) as electrolyte.[2,13] If the rate-controlling step is step 2, the potential dependence of the rate of reaction is similar to that observed for processes controlled by the rate of electron transfer. However, the apparent transfer coefficient has a very different meaning and depends greatly on the nature of the ions in the environment of the electrode. On the basis of existing double-layer data, changing the nature of the electrode in a given solution should result in a small decrease in the rate of the forward reaction; this follows from the fact that the charge on the electrode decreases at constant potential with increasing In content in the electrode,[9] and on going from the Hg system to the In–Ga system.[10,11] On the other hand, the rate of the reverse reaction should be markedly affected by the change in electrode material. Since the alkali metal is less solvated in the indium amalgam, the energy barrier for transfer from the metal to the electrode is reduced.

The above analysis is supported by the kinetic data obtained for the electroreduction of Li^+ from DMF solutions containing 0.1 mol dm^{-3} TBAP. When these data are plotted on a potential scale defined by the standard potential for the process at Hg, it is clear that rate constants measured for the forward process lie on one Tafel line independent of the nature of the electrode (fig. 5). This result reflects the fact that the apparent transfer coefficient does not depend greatly on the nature of the electrode. Tafel lines for the reverse reaction were drawn assuming that the apparent transfer coefficient for the reverse process β_a is given by $1-\alpha_a$. The dependence of the free energy of activation of the reverse process on the nature of the electrode is readily apparent.

The potential dependence of the rate of Na^+ reduction in DMF containing 0.25 mol dm^{-3} TEAP was investigated over a wide potential range (*ca.* 150 mV) by a.c. polarography using de Levie's analysis[14] to obtain the sum of the forward and backward rate constants and, hence, the forward rate constant using the relationship

$$\bar{k}_f/\bar{k}_b = \exp(-nf\eta) \quad (2)$$

where $\bar{k}_f$ and $\bar{k}_b$ are the overall rate constants for the forward and reverse reactions, respectively, n is the number of electrons involved ($n = 1$), η is the overpotential and $f = F/RT$. It is obvious from these data that the apparent transfer coefficient is potential dependent, decreasing from a value of *ca.* 0.6 at positive overpotentials to less than 0.2 at the most negative overpotential (fig. 6). Furthermore, standard rate data for reduction of Na^+ at dilute indium amalgams fall on the same curve when the potential scale is defined with respect to the standard potential of the system

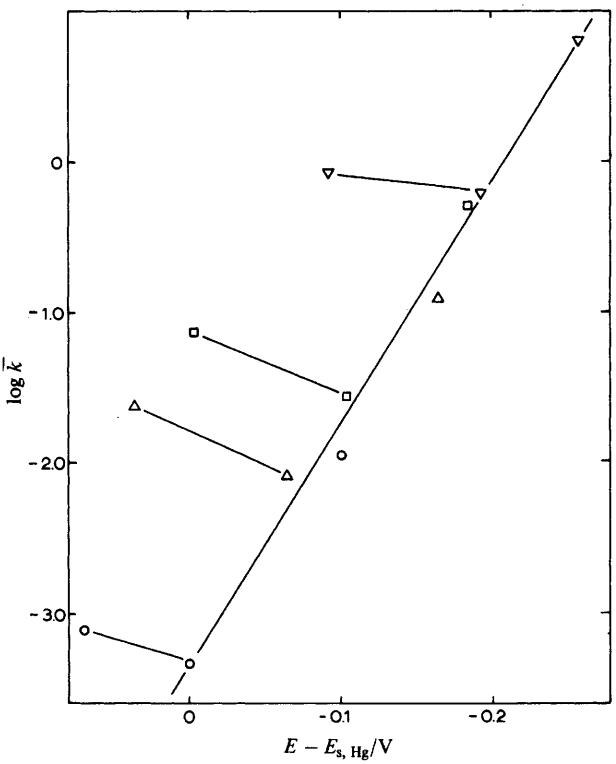

FIG. 5.—Plots of the logarithm of the rate constant for electroreduction of Li^+ in DMF at the standard potential and at a more cathodic potential against electrode potential measured with respect to the standard potential for the process at a Hg electrode. log k is also shown for the oxidation of Li at a potential anodic of the standard potential. The data were obtained at four different electrodes, namely, Hg (○), 15 at. % In–Hg (△), 30 at. % In–Hg (□) and 60 at. % In–Hg (▽). The electrolyte was 0.1 mol dm^{-3} TBAP.

$Na^+ + e \rightleftharpoons Na(Hg)$. These results indicate that the double-layer structure is virtually the same at Hg and dilute In amalgams at a given electrode potential. Although the comparison should be made in DMF, the result is not surprising considering the corresponding double-layer data in aqueous solution.[9]

The non-linear dependence of ln $\bar{k}_f$ on electrode potential can be analysed further on the basis of the model proposed above with three barriers involved in the overall electrode process (fig. 7). It can be shown that for a steady state with respect to transfer of the reactant through the double layer, the net forward rate constant is given by

$$\bar{k}_f = Z\left[\exp\left(\frac{\Delta G_1^{\neq}}{RT}\right) + \exp\left(\frac{\Delta G_2^{\neq}}{RT}\right) + \exp\left(\frac{\Delta G_3^{\neq}}{RT}\right)\right]^{-1} \quad (3)$$

where Z is the collision frequency and $\Delta G_i^{\neq}$ is the free energy of activation for step i that would obtain if the free energy of the initial state is the same as state A (this equation is derived in the Appendix). The effective free energy of activation is therefore

$$\Delta G_f^{\neq} = \boldsymbol{RT} \ln \left[\exp\left(\frac{\Delta G_1^{\neq}}{\boldsymbol{RT}}\right) + \exp\left(\frac{\Delta G_2^{\neq}}{\boldsymbol{RT}}\right) + \exp\left(\frac{\Delta G_3^{\neq}}{\boldsymbol{RT}}\right)\right]. \quad (4)$$

On the basis of the previous analysis, the height of barrier 1 is practically potential independent. On the other hand, the heights of the second and third barriers decrease

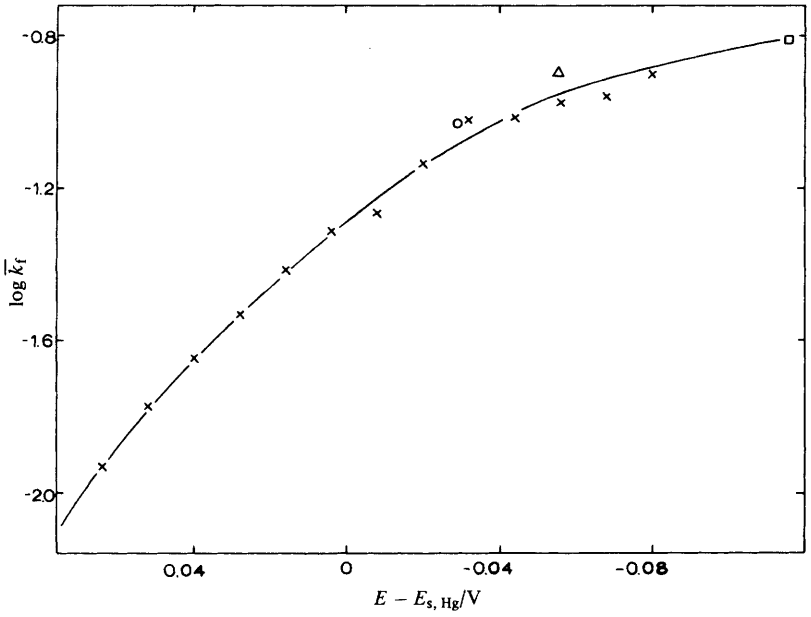

FIG. 6.—Plot of the logarithm of the rate constant for electroreduction of Na^+ in DMF with 0.25 mol dm^{-3} TEAP at Hg against the electrode potential measured with respect to the standard potential on Hg. Standard rate constants for the same process in the same media but at 3.5 at. % In–Hg (○), 7 at. % In–Hg (△) and 15 at. % In–Hg (□) are shown on the same potential scale.

as the potential is made more negative. Eventually, the process is controlled by barrier 1 and the forward rate constant becomes potential independent reaching a limiting value $\bar{k}_{\lim}$ given by

$$\bar{k}_{\lim} = Z \exp\left(-\Delta G_1^{\neq}/\boldsymbol{RT}\right). \quad (5)$$

The apparent transfer coefficient is given by

$$\alpha_a = \frac{\partial \Delta G_f^{\neq}}{\boldsymbol{F}\partial\phi^{md}} = \frac{\bar{k}_f}{Z}\left[\lambda_2 \exp\left(\frac{\Delta G_2^{\neq}}{\boldsymbol{RT}}\right) + \lambda_3 \exp\left(\frac{\Delta G_3^{\neq}}{\boldsymbol{RT}}\right)\right] \quad (6)$$

where ϕ^{md} is the potential drop across the inner layer and $\lambda_i = \partial \Delta G_i^{\neq}/\boldsymbol{F}\partial\phi^{md}$. On the basis of the above discussion λ_1 is assumed to be zero.[2] Furthermore, one may assume that $\exp(\Delta G_3^{\neq}/\boldsymbol{RT}) \ll \exp(\Delta G_1^{\neq}/\boldsymbol{RT}) + \exp(\Delta G_2^{\neq}/\boldsymbol{RT})$. Then, combining eqn (3), (5) and (6), it is easily shown that

$$\alpha_a \simeq \lambda_2 - \frac{\lambda_2 \bar{k}_f}{\bar{k}_{\lim}}. \quad (7)$$

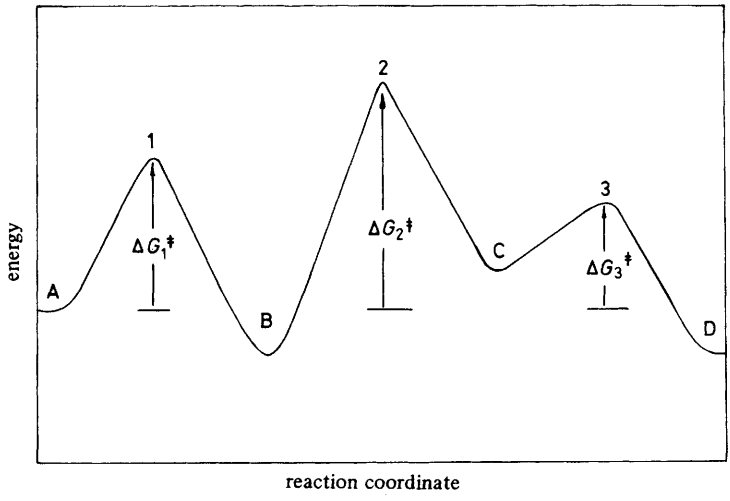

FIG. 7.—Potential energy profile for the process A → D with intermediates B and C and barriers 1, 2 and 3. The free energies of activation $\Delta G_1^{\neq}$, $\Delta G_2^{\neq}$ and $\Delta G_3^{\neq}$ are defined with respect to the initial state A.

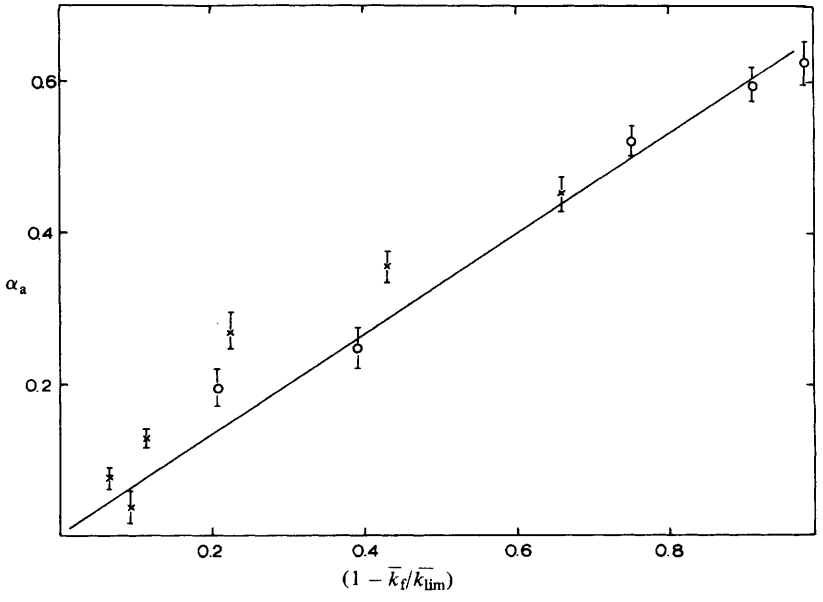

FIG. 8.—Plot of the apparent transfer coefficient α_a against $(1-\bar{k}_f/\bar{k}_{lim})$ where $\bar{k}_f$ is the net forward rate constant and $\bar{k}_{lim}$ its limiting (maximum) value. The data are for the electroreduction of Li^+ in AN (○) and Na^+ in DMF (×) at a variety of In amalgam electrodes.

Kinetic data for the reduction of Li^+ in AN and Na^+ in DMF are presented in fig. 8 according to eqn (7), that is, as a plot of α_a against $(1-\bar{k}_f/\bar{k}_{lim})$. It is apparent that a reasonable correlation is obtained, the scatter being due chiefly to errors in the experimental values of α_a. In addition, there is some uncertainty that a limiting value for the standard rate constant for reduction of Li^+ was reached, the value chosen being the highest value observed (0.68 cm s^{-1}). The slope of the plot gives the value of λ_2

(*ca.* 0.7). λ_2 is the fraction of the potential drop across the inner layer ϕ^{md} experienced in transfer from position A near the outer Helmholtz plane to position 2, the activation site for adsorption of the alkali metal. One expects this fraction to be rather large and to reflect the limiting apparent transfer coefficient at positive overpotentials. In view of the data presented in fig. 6, the value obtained here for λ_2 is quite reasonable and gives further support to the proposed mechanism.

In conclusion, the present data provide excellent support of the model for alkali metal electroreduction at liquid metals proposed earlier.[2] It is unfortunate that this model could not be tested more extensively. However, since changing the nature of the electrode to one in which the product is less strongly solvated results in reaction acceleration, one soon reaches the limits of the present experimental techniques. It is of interest to extend these studies to other amalgam-forming metal/metal ion systems. Work in this direction is currently in progress in this laboratory.

The financial support of the Natural Sciences and Engineering Research Council of Canada is gratefully acknowledged.

APPENDIX

We consider a process

$$A \rightarrow D \tag{A 1}$$

which is assumed to involve intermediates B and C and three free energy barriers denoted 1, 2 and 3 (fig. 7). The overall rate of the process is given by

$$v = \bar{k}_f[A] - \bar{k}_b[D] \tag{A 2}$$

where $\bar{k}_f$ and $\bar{k}_b$ are net forward and backward rate constants, respectively. At a steady state, the rate at which the system crosses each of the barriers is equal to the overall rate; thus, we may write

$$v = k_{f1}[A] - k_{b1}[B] \tag{A 3}$$

$$v = k_{f2}[B] - k_{b2}[C] \tag{A 4}$$

$$v = k_{f3}[C] - k_{b3}[D] \tag{A 5}$$

where k_{fi} and k_{bi} are the forward and backward rate constants for passage over the barrier i, respectively. On the basis of eqn (A 3) and (A 4), it is easily shown that

$$[B] = \frac{k_{f1}[A] + k_{b2}[C]}{k_{f2} + k_{b1}}. \tag{A 6}$$

Similarly, from eqn (A 4) and (A 5)

$$[C] = \frac{k_{f2}[B] + k_{b3}[D]}{k_{f3} + k_{b2}}. \tag{A 7}$$

Substituting eqn (A 7) into (A 6), one obtains an expression for [B] in terms of [A] and [D] and the various rate constants:

$$[B] = \frac{k_{f1}(k_{b2} + k_{f3})[A]}{(k_{b2} + k_{f3})(k_{f2} + k_{b1}) - k_{b2}k_{f2}} + \frac{k_{b2}k_{b3}[D]}{(k_{b2} + k_{f3})(k_{f2} + k_{b1}) - k_{b2}k_{f2}}. \tag{A 8}$$

Substitution of eqn (A 8) into (A 3) gives an expression for the rate of reaction in terms of [A] and [D] and the individual rate constants. When this expression is compared with that defining the rate on the basis of net rate constants [eqn (A 2)], one can write the following expressions for $\bar{k}_f$ and $\bar{k}_b$:

$$\bar{k}_f = \frac{k_{f1}k_{f2}k_{f3}}{k_{f3}k_{f2} + k_{f3}k_{b1} + k_{b1}k_{b2}} \tag{A 9}$$

and

$$\bar{k}_b = \frac{k_{b1}k_{b2}k_{b3}}{k_{f3}k_{f2} + k_{f3}k_{b1} + k_{b1}k_{b2}}. \tag{A 10}$$

Assuming that each rate constant may be expressed as

$$k_i = Z \exp(-\Delta G_i^{\neq}/RT)$$

where $\Delta G_i^{\neq}$ is the free energy of activation for process i and Z is the collision frequency, it can easily be shown that

$$\bar{k}_f = Z[\exp(\Delta G_1^{\neq}/RT) + \exp(\Delta G_2^{\neq}/RT) + \exp(\Delta G_3^{\neq}/RT)]^{-1}. \quad \text{(A 11)}$$

The free energies $\Delta G_1^{\neq}$, $\Delta G_2^{\neq}$ and $\Delta G_3^{\neq}$ are defined in fig. 7. Note that $\Delta G_2^{\neq}$ and $\Delta G_3^{\neq}$ are not the free energies of activation for passage of the reacting system over barriers 2 and 3 but instead are the free energies of activation for the processes that would obtain if the free energy of the initial state is the same as that in state A.

[1] A. S. Baranski and W. R. Fawcett, *J. Electroanal. Chem.*, 1978, **94**, 237.
[2] A. S. Baranski and W. R. Fawcett, *J. Chem. Soc., Faraday Trans. 1*, 1980, **76**, 1962.
[3] R. Parsons, *Surf. Sci.*, 1964, **2**, 418.
[4] A. N. Frumkin, *J. Electroanal. Chem.*, 1965, **9**, 1973.
[5] A. Baranski and Z. Galus, *J. Electroanal. Chem.*, 1973, **46**, 289.
[6] P. Delahay, *Double Layer and Electrode Kinetics* (Wiley-Interscience, New York, 1965), chap. 9.
[7] A. N. Frumkin, *Potentials of Zero Charge* (Nauka, Moscow, 1979), chap. 8.
[8] W. R. Fawcett, *Isr. J. Chemistry*, 1979, **18**, 3.
[9] E. V. Yakovleva and N. V. Nikolaeva-Fedorovich, *Elektrokhimiya*, 1970, **6**, 35.
[10] I. A. Bagotskaya, S. A. Fateev, N. B. Grigor'ev and A. N. Frumkin, *Elektrokhimiya*, 1973, **9**, 1676.
[11] L. M. Dubova and I. A. Bagotskaya, *Elektrokhimiya*, 1977, **13**, 64.
[12] K. Izutsu, S. Sakura, K. Kuroki and T. Fujinaga, *J. Electroanal. Chem.*, 1971, **32**, 11.
[13] K. Izutsu, S. Sakura and T. Fujinaga, *Bull. Chem. Soc. Jpn*, 1972, **45**, 445.
[14] R. de Levie and A. A. Husovsky, *J. Electroanal. Chem.*, 1969, **22**, 29.

(PAPER 1/1021)